

this and other studies<sup>34–37</sup> that the process of transcription activation involves at least two independent, but interrelated steps. The initial step involves the removal of molecules that maintain genes in a silent state, a process known as antirepression<sup>36</sup>. The second step represents true activation, in which the levels of

expression of particular genes are increased well above basal levels. It is likely that these distinct events are coupled and that a family of ubiquitous activators operates to remove repressors, thereby setting specific genes into a state responsive to gene-specific activators. □

Received 24 March; accepted 28 July 1993.

1. Ptashne, M. & Gann, A. F. *Nature* **346**, 329–331 (1990).
2. Zavel, L. & Reinberg, D. *Progress in Nucleic Acid Research and Molecular Biology* Vol. 44 (eds Cohn, W. E. & Moldave, K.) 67–108 (Academic, San Diego, 1993).
3. Lin, Y.-S., Ha, I., Maldonado, E., Reinberg, D. & Green, M. R. *Nature* **353**, 569–571 (1991).
4. Ingles, C. J., Shales, M., Cress, W. D., Triezenberg, S. J. & Greenblatt, J. *Nature* **351**, 588–590 (1991).
5. Roberts, S. G. E., Ha, I., Maldonado, E., Reinberg, D. & Green, M. R. *Nature* **363**, 741–744 (1993).
6. Lin, Y.-S., Carey, M. F., Ptashne, M. & Green, M. R. *Cell* **54**, 659–664 (1988).
7. D'Arpa, P. et al. *Proc. natn. Acad. Sci. U.S.A.* **85**, 2543–2547 (1988).
8. Liu, L. F. & Miller, K. G. *Proc. natn. Acad. Sci. U.S.A.* **78**, 3487–3491 (1981).
9. Madden, K. R. & Champoux, J. J. *Cancer Res.* **52**, 525–532 (1992).
10. Eng, W., Pandit, S. D. & Sternglanz, R. J. *biol. Chem.* **164**, 13373–13376 (1989).
11. Lynn, R. M., Bjornsti, M., Caron, P. R. & Wang, J. C. *Proc. natn. Acad. Sci. U.S.A.* **86**, 3559–3563 (1989).
12. Wang, J. A. *Rev. Biochem.* **54**, 665–697 (1985).
13. Weis, L. & Reinberg, D. *FASEB J.* **6**, 3300–3309 (1992).
14. Cortes, P., Flores, O. & Reinberg, D. *Molec. cell. Biol.* **12**, 413–421 (1992).
15. Zhou, Q., Lieberman, P. M., Boeyer, T. G. & Berk, A. J. *Genes Dev.* **6**, 1964–1974 (1992).
16. Buratowski, S., Hahn, S., Guarente, L. & Sharp, P. A. *Cell* **56**, 549–561 (1989).
17. Maldonado, E., Ha, I., Cortes, P., Weis, L. & Reinberg, D. *Molec. cell. Biol.* **10**, 6335–6347 (1990).
18. Berger, S. L. et al. *Cell* **70**, 251–265 (1992).
19. Kelleher, R. J. I., Flanagan, P. M. & Kornberg, R. D. *Cell* **61**, 1209–1215 (1990).
20. Lewin, B. *Cell* **61**, 1161–1164 (1990).
21. Gill, G. & Tjian, R. *Curr. Opin. Genet. Dev.* **2**, 236–242 (1992).
22. Seto, E. et al. *Proc. natn. Acad. Sci. U.S.A.* **89**, 12028–12032 (1992).
23. Mack, D. H., Vartikar, J., Pipas, J. M. & Laimins, L. A. *Nature* **363**, 281–283 (1993).
24. Choder, M. *Genes Dev.* **5**, 2315–2326 (1991).
25. Fleischmann, G. et al. *Proc. natn. Acad. Sci. U.S.A.* **81**, 6958–6962 (1984).
26. Stewart, A. F., Herrera, R. E. & Nordheim, A. *Cell* **60**, 141–149 (1990).
27. Liu, L. F. & Wang, J. C. *Proc. natn. Acad. Sci. U.S.A.* **84**, 7024–7027 (1987).
28. Thrash, C., Bankier, A. C., Barrel, B. G. & Sternglanz, R. *Proc. natn. Acad. Sci. U.S.A.* **82**, 4374–4378 (1985).
29. Goto, T. & Wang, J. C. *Proc. natn. Acad. Sci. U.S.A.* **82**, 7178–7182 (1985).

30. Lee, P. L., Brown, S. D., Chen, A. & Hsieh, T.-H. *Proc. natn. Acad. Sci. U.S.A.* **90**, 6656–6660 (1993).
31. Inostroza, J. A., Mermelstein, F. H., Ha, I., Lane, W. S. & Reinberg, D. *Cell* **70**, 477–489 (1992).
32. Meisterernst, M. & Roeder, R. G. *Cell* **67**, 557–567 (1991).
33. Meisterernst, M., Roy, A. L., Lieu, H. M. & Roeder, R. G. *Cell* **66**, 981–993 (1991).
34. Laybourn, P. J. & Kadonaga, J. K. *Science* **254**, 238–245 (1991).
35. Workman, J. L., Taylor, I. C. A. & Kingston, R. E. *Cell* **64**, 533–544 (1991).
36. Croston, G. E., Kerrigan, L. A., Lira, L. M., Marshak, D. R. & Kadonaga, J. T. *Science* **151**, 643–649 (1991).
37. Croston, G. E., Laybourn, P. J., Paranjape, S. M. & Kadonaga, J. T. *Genes Dev.* **6**, 2270–2281 (1992).
38. Lu, H., Flores, O., Weinmann, R. & Reinberg, D. *Proc. natn. Acad. Sci. U.S.A.* **88**, 10004–10008 (1991).
39. Chasman, D. I., Leatherwood, J., Carey, M., Ptashne, M. & Kornberg, R. D. *Molec. cell. Biol.* **9**, 4746–4749 (1989).
40. Lillie, J. W. & Green, M. R. *Nature* **338**, 39–44 (1989).
41. Tanese, N., Pugh, B. F. & Tjian, R. *Genes Dev.* **5**, 2212–2224 (1991).
42. Ha, I., Lane, W. S. & Reinberg, D. *Nature* **352**, 689–695 (1991).
43. Shuman, S. J. *biol. Chem.* **266**, 1796–1803 (1991).
44. Srivenugopal, K. S., Lockshon, D. & Morris, D. R. *Biochemistry* **23**, 1899–1906 (1984).
45. Liu, F. & Green, M. R. *Cell* **61**, 1217–1224 (1990).
46. Merino, A., Buckbinder, L., Mermelstein, F. H. & Reinberg, D. *J. biol. Chem.* **264**, 21266–21276 (1989).
47. Pugh, B. F. & Tjian, R. *Cell* **61**, 1187–1197 (1990).

ACKNOWLEDGEMENTS. We thank R. Drapkin, K. J. Mariani, L. Liu, M. Green, R. Sternglanz and L. Zavel for discussion and comments on the manuscript, S. Shuman, K. J. Mariani and J. Hurwitz for the gifts of vaccinia virus, *E. coli* and human DNA topoisomerases I, respectively, M. Bjornsti and J. Wang for the yeast topoisomerase I, A. Berk for sharing before publication the cell line expressing eTFIID, R. Tjian and M. Green for the GAL4 derivative proteins and their expression vectors, M. Carey for the plasmid pG5MLT, the members of the laboratory for discussions and ideas while the work was in progress, and R. Robinson for technical assistance. This work was supported by grants from the NIH to D.R.; A.M. is the recipient of the Kirin Brewery Fellowship and D.R. is a recipient of an American Cancer Society Faculty Research Award. This article is dedicated to the memory of Dr Josef Aloni.

## LETTERS TO NATURE

### Supernova 1993J as a spectroscopic link between type II and type Ib supernovae

D. A. Swartz\*, A. Clocchiatti†, R. Benjamin†, D. F. Lester† & J. C. Wheeler†

\* Space Science Laboratory, NASA Marshall Space Flight Center, Huntsville, Alabama, USA

†Department of Astronomy, University of Texas at Austin, RLM 15.308, Austin, Texas 78712-1083, USA

SUPERNOVA 1993J in the nearby galaxy M81 is one of the closest—and hence brightest—supernovae to be witnessed this century. The early spectrum of SN1993J showed<sup>1–3</sup> the characteristic hydrogen signature of type II supernovae, but its subsequent evolution is atypical for this class of supernova. Here we present optical and infrared spectra of SN1993J up to 43 days after outburst, which reveal the onset of the helium absorption and emission features more commonly associated with hydrogen-free type Ib supernovae. Corresponding model spectra show that the progenitor star must have possessed an unusually thin (for type II supernovae) hydrogen-rich envelope overlying a helium-rich mantle. Moreover, the supernova ejecta must have remained compositionally stratified, with little transport of the hydrogen-rich material down into the underlying helium layer, or mixing of heavier elements (such as radioactive <sup>56</sup>Ni) outwards. SN1993J therefore represents a transitional object between hydrogen-dominated type II supernovae, and hydrogen-free, helium-dominated type Ib supernovae.

Optical spectra of SN1993J taken at 5:30 UT on 29 April and 4:05 on 9 May 1993 are shown in Fig. 1 together with a spectrum

taken 20 April 1993 (ref. 1). These correspond to 32, 43 and 23 days, respectively, after the explosion (assuming that shock break-out occurred 28 March<sup>2</sup>). All spectra show the hydrogen Balmer series in absorption. The spectrum of 20 April, in which the helium features are weak or absent, shows an apparent flat-topped H $\alpha$  profile in both absorption and emission. Between 20 and 29 April He I lines appeared as reported earlier<sup>3</sup>. The time for this event is probably constrained more closely by the changes in the shape of the Na I 5893-Å line observed between 22 and 26 April<sup>4</sup> as the He I 5876 absorption became stronger. After the helium lines become prominent, the He I 6678-Å line appears on the flat-topped H $\alpha$  emission feature. The strength of the helium absorption lines increased in comparison to the strength of the hydrogen features in the ~10 days elapsed between 29 April and 9 May. Further details of the observed spectra are presented in Table 1.

Infrared spectra shown in Fig. 2 were taken at 3:50 on 3 May 1993 (37 days after shock break-out). The spectrum shows He I 1.083- $\mu$ m emission with a normal P-Cygni profile, and weak He I 2.058- $\mu$ m emission with an asymmetric absorption trough. Hydrogen (Paschen) Pa- $\beta$  1.282- $\mu$ m emission is observed with a flat-topped P-Cygni profile.

Figures 1 and 2 also present the results of a model atmosphere of the supernova at 40 days after explosion. The model is derived from the unmixed 4.0- $M_{\odot}$  (solar masses) hydrodynamic model of Shigeyama *et al.*<sup>5</sup>. In this model, the supernova is originally compact, lacking an extended hydrogen-rich envelope, and hence the model will not reproduce the observed initial peak of the SN1993J light curve<sup>2</sup>; but comparison with dynamical models with low-mass extended envelopes show that it is a reasonable representation of the density structure at later times.

The parameters that we varied to obtain the best agreement with the observations are: the mass assigned to the hydrogen-

TABLE 1 Velocities at absorption minima (km s<sup>-1</sup>)

Transition	Velocity on date	
	29 April	9 May
H $\alpha$	-10,362	-9,790
H $\beta$	-8,375	-8,714
H $\gamma$	-8,372	-8,704
H $\delta$ *	-8,619	-9,430
He I 4,471 Å	?	-5,552
He I 4,921 Å	-5,577	-5,531
He I 5,015 Å	-5,434	-5,434
He I 5,876 Å	-7,316	-7,224
He I 6,678 Å†	-6,940	-6,496
He I 7,065 Å‡	?	-7,010
He I 7,281 Å§	?	-5,217
Ca II 8,438, 8,542, 8,662 Å	-6,197	-5,544
Fe II 4,925 Å¶		-7,785
Fe II 5,020 Å¶		-7,817

\* Blended with Ca H & K, and possibly with He I 4,026 Å.

† Blended with Na I 5,893 Å.

‡ Blended with the telluric oxygen band at 6,870 Å.

§ Blended with the telluric H<sub>2</sub>O band at 7,280 Å.

|| Mean value of 8,438-Å and 8,542-Å absorption.

¶ Measured on spectrum of 20 April, before the onset of He I 4,921 Å, and He I 5,015 Å.

TABLE 2 Theoretical model parameters

Mass at core collapse	4.00 $M_{\odot}$
Total ejecta mass	2.45 $M_{\odot}$
Total $^{56}\text{Ni}$ mass	0.08 $M_{\odot}$ ( $v < 2,700 \text{ km s}^{-1}$ )
Total luminosity	$7.8 \times 10^{41} \text{ ergs s}^{-1}$ (at 40 days)
Photosphere position*	$9.2 \times 10^{14} \text{ cm}$ ( $v = 2,650 \text{ km s}^{-1}$ )

Layer	Mass ( $M_{\odot}$ )	$v_{\text{max}}$ (km s $^{-1}$ )	$X_{\text{e}}^{\dagger}$
Heavy metal	0.30	2,600	0.42
Oxygen	0.47	3,200	0.20
Helium	1.40	7,500	0.04
Hydrogen/helium	0.40	11,600	0.14

Abundances (in $M_{\odot}$ )							
H	0.04	C	0.07	Mg	0.05	Ca	0.01
He	1.66	O	0.47	Si	0.09	Fe	0.06
		Na	0.00	S	0.05		

\* Corresponding to electron scattering of optical depth unity.

† Average ionization fraction.

rich outer layer; the H/He ratio,  $X$ , in this layer (plus solar metals); the mass and distribution of radioactive  $^{56}\text{Ni}$  produced in the explosion; the mixing of the ejecta (independent of the  $^{56}\text{Ni}$  distribution); the total ejecta mass; and the maximum ejecta velocity. Model details are given in Table 2 and a discussion of the general supernova atmosphere calculations are presented elsewhere<sup>6</sup>.

Two conditions are necessary for emission lines to form: the electron density must be low<sup>7</sup> to avoid electron quenching and substantial  $\gamma$ -ray heating of the regions containing helium must occur<sup>6</sup>. The helium lines become visible after (1) the ionized outer H/He layer recombines, allowing exposure of the underlying helium mantle; (2) increasing  $\gamma$ -ray heating of the helium layer; and (3) the free-electron density in the mantle has declined sufficiently because of expansion and cooling. The mass adopted here for the H/He envelope, 0.4  $M_{\odot}$ , with  $X=0.1$ , seems to produce the correct chronology and to fit the spectrum. Larger envelope masses have not been ruled out at this stage, but a smaller envelope mass would lead to premature helium line emission. The spectrum is not very sensitive to the H/He ratio in the outermost layer at 40 days; only subtle changes in the line strengths were encountered on varying the H/He mass ratio in this layer from 1/9 to 9/1.

The radioactive material cannot be accelerated to large velocities without generating excessively strong hydrogen and helium emission lines from the outermost layers. Moreover, the initial  $^{56}\text{Ni}$  mass cannot be large, independent of distribution; models with  $M_{\text{Ni}}=0.15 M_{\odot}$  resulted in nearly fully ionized hydrogen and a continuum optical depth of unity at the base of the H/He layer at 40 days, inconsistent with the spectrum. The initial mass of  $^{56}\text{Ni}$  was therefore more likely to be  $\leq 0.1 M_{\odot}$ . The remaining elements cannot be mixed without contaminating the spectrum with strong 'metal' lines, particularly [Ca II] and [O I], as can be seen by comparing the mixed and unmixed model spectra of Swartz *et al.*<sup>6</sup>. The 6.0- $M_{\odot}$  and 3.0- $M_{\odot}$  models of Shigeyama *et al.*<sup>5</sup> have expansion velocities that are slightly too low and too high, respectively. The original 4.0- $M_{\odot}$  model<sup>5</sup> contains about 0.04  $M_{\odot}$  of ejecta expanding with  $v > 12,000$  km s<sup>-1</sup>. This is still faster than the velocities inferred from the hydrogen- and helium-line absorption minima, but if this layer is omitted the broad red wings of the helium emission lines are not reproduced. Moreover, O I 7,774-Å [O I] 6,300-Å, and [O I] 5,577-Å emission lines are formed in the relatively hot, low-density helium and H/He layers at 40 days, and a better fit to the O I 7,774-Å feature is possible with this outermost, low-density material included. The interaction of the supernova

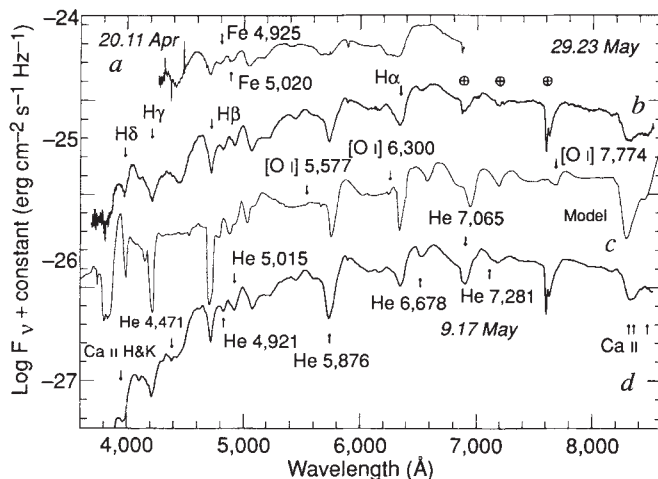


FIG. 1 Optical spectra of SN1993J. From top to bottom, the different curves are (a) The observed spectrum of SN1993J on 20 April<sup>1</sup> (thin line), (b) the spectrum observed at 5:30 UT on 29 April (thick line), (c) the synthetic model spectrum described in the text (thin line), (d) the spectrum observed at 4:05 UT on 9 May (thick line). The absolute fluxes ( $F$ ) of the model were reddened using a mean absorption law, scaled to absorption in the visible ( $A_V=0.45$ ). The flux scale of all spectra was arbitrarily shifted for clarity. Observations were made using the Image Grism Instrument (IGI) in spectroscopic configuration on the McDonald Observatory 2.1-m (29 April) and 0.76-m (9 May) telescopes. Feige 34 (ref. 20) HD84937, and BD+262606 (ref. 21) were used for flux calibration. The overall slopes of both spectra are systematically distorted by atmospheric differential refraction losses<sup>22</sup> with greater loss of light in the blue portion of the observed spectra. The wavelength scale of the observed spectra has not been corrected for the motion of NGC 3031 ( $-49 \pm 10$  km s<sup>-1</sup>, ref. 23). The arrows and labels close to them mark the position of blueshifted absorptions of selected lines. The Earth symbols mark the position of three strong telluric absorption features due to oxygen and water molecules.

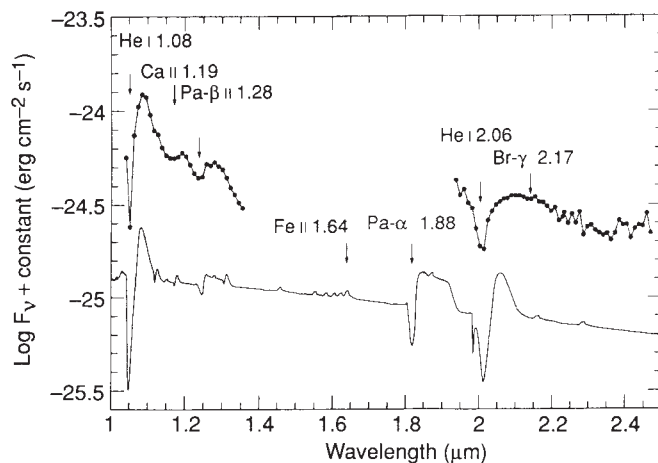


FIG. 2 Comparison of the 3 May infrared spectrum of SN1993J with the model from Fig. 1. The upper curves are the observed spectra; the solid line is the theoretical spectrum described in the text. The vertical scale indicates the flux level of the observed data, with the theoretical spectrum offset by a constant for clarity. The observations were made with the McDonald Observatory Infrared Grating Spectrometer on the 2.7-m telescope. This spectrometer is described further by Lester *et al.* (ref. 24). Spectra were taken with a low resolution grating covering the J-band (resolution  $\approx 100$ ) and the K-band (resolution  $\sim 200$ ). BS3888 (spectral type F2IV) was used for flux calibration and flat fielding assuming  $J=3.24$ ,  $K=2.99$ , and a colour temperature of 6,700 K for the standard. The seeing and transparency were good but the small beam-size, combined with guiding errors, limit the absolute flux calibration to about 15%. The signal-to-noise ratio (S/N) is estimated to be  $\approx 30$  except towards the ends of the atmospheric windows. The region  $\lambda > 2.2 \mu\text{m}$  has lower S/N ( $\approx 15$ ). The blueshift from He I 1.083  $\mu\text{m}$  is uncertain because the location of the minimum is sensitive to corrections for atmospheric absorption. The feature at  $\lambda \sim 1.19 \mu\text{m}$  could be Ca II lines at 1.1836 and 1.1947  $\mu\text{m}$ . The model gives approximately the correct flat-top profile for Pa- $\beta$  while Bracket- $\gamma$  is negligible. The theoretical model predicts that the He I 2.058- $\mu\text{m}$  line should show a standard P-Cygni line profile, as do both the observations and model for He I 1.083  $\mu\text{m}$ . The lack of distinct emission in the He I 2.058- $\mu\text{m}$  observation may be due to blending with other lines not included in the model spectrum, but we note that the emission at 2.058  $\mu\text{m}$  was also relatively small in SN1987A. (The notch at 1.98  $\mu\text{m}$  arises from He I in the outermost zone of the model.) Arrows and symbols have the same meaning as in Fig. 1.

ejecta with a pre-existing stellar wind from the progenitor star has not been considered here, but the fact that the models favour a relatively low terminal velocity and can still tolerate a hot outermost layer, is consistent with wind-interaction models<sup>8,9</sup>.

The subsequent spectral evolution of SN1993J can be estimated from these models. Over the first 100 to 150 days, Ca II and O I lines will be relatively weak and narrow relative to typical SN Ic's such as SN1987M (ref. 10) in the absence of mixing<sup>6</sup>. The optical helium lines will remain until  $\sim 100$  days after explosion, but fade by about 200 days. H $\alpha$  and H $\beta$  should be seen in absorption with weak H $\alpha$  emission for the first 100 days and should then also fade in the next 100 days.

The basic parameters of our model, deduced from the emergence of the helium in the spectrum—an ejecta mass, of  $\sim 2 M_{\odot}$  and an outer layer of  $\sim 0.4 M_{\odot}$  with a hydrogen mass fraction of  $X \approx 0.1$  and a  $^{56}\text{Ni}$  mass of  $\leq 0.1 M_{\odot}$ —are similar to, but independent of, constraints from the light curve<sup>2,11–13</sup> (but see ref. 14) and independent of the distance to the supernova and reddening because our results are based on modelling the spectrum and not the light curve. The  $^{56}\text{Ni}$  mass is constrained in our model by the degree of ionization independent of the distance to SN1993J.

The helium lines in SN1993J are similar to those observed in the type Ib supernova 1984L (ref. 7) but the latter never devel-

oped hydrogen lines. This strongly suggests that SN1993J is a transition object between ordinary (plateau) type II supernovae, which retain a massive hydrogen envelope with an approximately solar abundance of helium (although the helium does not show up distinctly in the optical spectrum), and type Ib supernova, which are helium-rich<sup>6,7,15</sup> but show no hydrogen at any stage of their evolution. The obvious interpretation is that mass loss of the hydrogen envelope went to completion in SN1984L and nearly to completion in SN1993J.

The spectral models predict that hydrogen and helium will no longer be observable after about 200 days. It is worth noting that the peculiar type II supernova SN1987K also showed evidence for hydrogen near maximum light but none at later times<sup>16</sup>. Moreover, closer inspection of the spectra shows that SN1987K may have begun to show lines of He I after its brightness maximum<sup>17</sup>. SN1987K may thus have been the first observed example of the class of supernovae represented by SN1993J although there are quantitative differences in the spectral developments of these two objects.

The spectral models of SN1993J also illustrate that even a small amount of hydrogen in the envelope will appear in the spectrum. This serves to emphasize that Type Ic events such as SN1987M were even more deficient in hydrogen than is SN1993J<sup>6</sup>, although they may contain a trace of hydrogen<sup>18,19</sup>. □

Received 20 May; accepted 9 August 1993.

- Trammell, S. R., Hines, D. C. & Wheeler, J. C. *Astrophys. J.* (in the press).
- Wheeler, J. C. *et al. Astrophys. J.* (in the press).
- Filippenko, A. V. & Matheson, T. *IAU Cir. No.* 5787 (1993).
- Hu, J. Y., Li, Z. W., Jiang, X. J. & Wang, L. F. *IAU Circ. No.* 5777 (1993).
- Shigeyama, T., Nomoto, K., Tsujimoto, T. & Hashimoto, M.-A. *Astrophys. J.* **361**, L23–L27 (1990).
- Swartz, D. A., Filippenko, A. V., Nomoto, K. & Wheeler, J. C. *Astrophys. J.* **411**, 313–322 (1993).
- Harkness, R. P. *et al. Astrophys. J.* **317**, 355–367 (1987).
- Fransson, C. *Astr. Astrophys.* **133**, 264–284 (1984).
- Harkness, R. P. & Wheeler, J. C. *Proc. astr. Soc. Aust.* **7**, 431–433 (1989).
- Filippenko, A. V., Porter, A. C. & Sargent, W. L. *Astr. J.* **100**, 1575–1587 (1990).
- Nomoto, K. *et al. Nature* (in the press).
- Woosley, S. E., Eastman, R. G., Weaver, T. A. & Pinto, P. A. *Astrophys. J.* (in the press).
- Podsiadlowski, Ph., Hsu, J. J. L., Joss, P. C. & Ross, R. R. *Nature* **364**, 509–511.
- Hoflich, P., Langer, N. & Duschinger, M. *Astr. Astrophys.* (in the press).

- Lucy, I. B. *Astrophys. J.* **383**, 308–313 (1991).
- Filippenko, A. V. *Astr. J.* **96**, 1941–1948 (1988).
- Filippenko, A. V., Matheson, T. & Ho, L. C. *Astrophys. J.* (in the press).
- Jeffery, D. J., Branch, D., Filippenko, A. V. & Nomoto, K. *Astrophys. J.* **377**, L89–L92 (1991).
- Filippenko, A. V. *Astrophys. J.* **384**, L37–L40 (1992).
- Stone, R. P. S. *Astrophys. J.* **218**, 767–769 (1977).
- Oke, J. B. & Gunn, J. E. *Astrophys. J.* **266**, 713–717 (1983).
- Filippenko, A. V. *Publ. astr. Soc. Pacif.* **94**, 715–721 (1982).
- de Vaucouleurs, G. *et al. Third Reference Catalogue of Galaxies* (Springer, New York, 1991).
- Lester, D. F., Carr, J., Joy, M. & Gaffney, N. *Astrophys. J.* **352**, 544–560 (1990).

ACKNOWLEDGEMENTS. We appreciate the donation of telescope time by D. Lambert, and efforts by the staff of the McDonald Observatory to incorporate SN1993J into the schedule. This research was supported in part by grants from the NSF, NASA and the R. A. Welch Foundation. D.A.S. is supported by a NAS/NRC Resident Research Associateship.